Site-selective XAFS: a new tool for catalysis research

F.M.F. de Groot

Department of Inorganic Chemistry, Sorbonnelaan 12, 3584 CA Utrecht, The Netherlands
E-mail: F.M.F.de Groot@chem.uu.nl

Site-selective X-ray absorption fine structure (XAFS) experiments will become an important tool in the study of active sites and metal–support interactions in catalysis. Site-selective XAFS is possible with the detection of specific X-ray emission channels. Selectivity can be obtained for the valence or for the nature of the neighbouring atoms. This opens a wide range of new experiments, for example with valence-selective XAFS the difference in local structure of an element present with two valences can be studied. With site-selective XAFS the local surroundings of a metal in contact with oxygen or carbon can be differentiated from the local surroundings of all the other metal atoms.

Keywords: XAFS, XANES, heterogeneous catalysis, resonant X-ray emission

1. Introduction

A major aim of catalysis research is to fully characterize the local environment of catalytically active centres and reaction intermediates formed during reactions. For a further understanding of catalysis at an atomic level, it is crucial to obtain information about the structure of the active site during reaction conditions and in the presence of the reacting molecules. Given the fact that most catalysts are disordered with structurally ill defined phases, one road to tackle this extremely complex problem is to prepare structurally well defined catalytic test systems. However, XAFS spectroscopy has shown in the last years that the structure of the catalyst, in particular the structure of the active site, is different in "real" catalysts at reaction temperatures. The state of the art *in situ* XAFS technique is now at a level that catalytic events can be followed at an atomic scale. Changes in inter-atomic potentials due to reacting molecules at distance of a few ångströms can be experimentally observed. This information will give valuable experimental input for the theoretical attempts to describe the active sites at an atomic level, based on realistic structural and electronic models. We will indicate three types of catalysts, for which site-selective XAFS could be an important new tool:

(i) the nickel nanoparticle of figure 1;

(ii) Pt, Pd and mixed metals supported on oxides (zeolites, silica) or carbon fibrils;

(iii) CoMo catalysts for hydrodesulphurization (HDS).

(i) Imagine a nickel nanoparticle sitting on an oxide support as sketched in figure 1. Three types of nickel atoms can be distinguished: (1) "bulk" nickel atoms in the interior of the nanoparticle and bonded only to other nickel atoms, (2) nickel atoms bonded to the oxygen of the support (dashed diagonally) and (3) nickel atoms bonded to carbon of a transition state (dashed horizontally). Normal

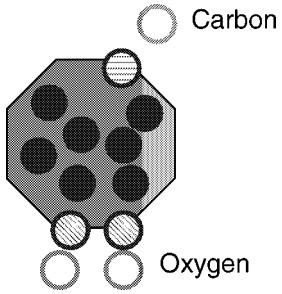

Figure 1. A nanoparticle with some of its atoms indicated. The horizontally shaded atom is the active site bonded to a carbon atom. The diagonally shaded atoms are bonded to oxygen of the support.

EXAFS, as well as most other characterization techniques, will yield a signal that will be a linear combination of all three sites. A technique that is able to distinguish these three types of metal atoms will add crucial additional information. In this paper it will be shown that EXAFS can be made sensitive to only those nickel atoms bonded to carbon. In addition, this so-called site-selective EXAFS can be performed *in situ* and time-resolved. Instead of nickel, any other 3d-metal nanoparticle can be studied in a completely analogous manner. If alloys are studied with site-selective XAFS performed at both metal edges, one could hope to determine which of the two metals is preferred as the active site and which metal is preferred as the bond to the support. Supported 3d-metal nanoparticles are used as catalysts in a very large range of catalytic reactions [1,2].

(ii) Pt and Pd supported on oxides or carbon fibrils are important catalytic systems for the improvement of combustion processes and the avoidance of polluting emissions. An important topic is the interaction of the metal particles/clusters with the support. The metal support interaction is likely to affect the distribution of cluster sizes and the electronic structure of promoters, and as such can be expected to have major effects on the catalytic properties. Recent research from the group has established that the

acidity of the support material affects the electronic structure of small (1 nm) metal particles as well as the catalytic activity [3,4].

(iii) CoMo (cobalt–molybdenum) catalysts are important for the hydrodesulphurization (HDS) and hydrocracking in large-scale oil refineries. Because of its major importance, this system has been intensively studied over the last decades. Still the atomic nature of the system and the detailed description of the catalytic process are only very approximately known. The catalyst consists of MoS_2 particles that are activated by Co promoter atoms. Using EXAFS, the position of the Co atoms has been found to be on the edges of the MoS_2 sheets, though this result is not uniformly accepted. The Co–MoS_2 particles are supported on oxides (silica, alumina, TiO_2) and the nature of the oxide–sulphide interaction has been an important topic of research within the group [5,6].

We will come back to these three systems at the end of the paper. First, in the next section, we start with some basic aspects of X-ray absorption and X-ray emission. It is this combination of X-ray absorption and X-ray emission that gives rise to a series of new experiments. Some of these new possibilities are discussed and the potential applications to catalysis research are highlighted.

2. Basic aspects of X-ray absorption and X-ray emission

X-ray absorption is a synchrotron-based characterization technique, which can be divided into near-edge spectroscopy (XANES) and extended X-ray absorption fine structure (EXAFS). In the X-ray absorption process, a core electron is excited to an empty state and, as such, X-ray absorption probes the unoccupied part of the electronic structure of the system [7]. In the EXAFS region, the excited electron has significant kinetic energy (E_e), which is related to the wave vector (k_e) as $E_e = (\hbar/2\pi)k_e^2$. The distances to the nearest neighbours are closely related to the Fourier transform of the wave vector. To perform a more accurate analysis, the EXAFS signal can be simulated with multiple scattering. This analysis yields for many systems the most accurate determination of the local geometry. The XANES structure can also be simulated with the multiple scattering formalism. Alternatively one can use electronic structure models such as molecular-orbitals or density-functional theory [8]. An important aspect of the usefulness of X-ray absorption is that one obtains element specific information. This also implies that if two or more types of atoms of a particular element are present, the X-ray absorption spectral shape is a linear combination of all individual sites. This aspect limits the usefulness of XANES and EXAFS in systems with atoms in a variety of sites. This problem can be partly solved with the use of site-selective XAFS as will be discussed below.

The X-ray absorption spectral shape is described with the Fermi Golden rule:

$$I_{\mathrm{XAS}} \approx \left|\left\langle \Phi_{\mathrm{f}}|\hat{e}r|\Phi_{\mathrm{i}}\right\rangle\right|^2 \delta_{E_{\mathrm{f}}-E_{\mathrm{i}}-\hbar\omega}. \tag{1}$$

The intensity is proportional to a dipole matrix element coupling the initial and final states. The delta function takes care of the conservation of energy. In the final state, a core electron has been excited and the final state can be described as the initial state with a "free" electron added and a core electron removed: $\Phi_{\mathrm{f}} = c\varepsilon\Phi_{\mathrm{i}}$. An important approximation is to assume that the matrix element can be rewritten into a single electron form by removing all "inactive" electrons (i.e., Φ_{i}). With this approximation, the series of delta functions identifies with the DOS (ρ) and the X-ray absorption spectral shape becomes

$$I_{\mathrm{XAS}} \approx \left|\left\langle \varepsilon|\hat{e}r|c\right\rangle\right|^2 \rho. \tag{2}$$

The dipole matrix element dictates that the DOS has an orbital moment that differs by one from the core state and, because in the final state a core hole is present, the DOS should be calculated with a core hole present. In many cases, this approximation gives an adequate simulation of the XAS spectral shape. In some cases though, the single particle approximation breaks down and the XANES structure is affected by the core wave function. This so-called multiplet effect will be discussed in some detail because it is an important effect that can be used to do selective XAFS.

The breakdown of the single particle model is important in systems with electrons in narrow bands, for example the 3d-metals or the rare earths. In these systems the core wave function strongly overlaps with the 3d-valence wave functions. This strong local interaction has to be considered in order to obtain an accurate description of the XANES spectral shape. A successful analysis method has been developed based on a crystal field multiplet model [9]. It offers a large sensitivity to the valence and the symmetry of the element studied. Figure 2 gives the crystal field multiplet calculation for MnO. The bottom of figure 2 gives the comparison between Mn^{2+}, Mn^{3+} and Mn^{4+}. The spectral shapes change considerably and 2p XAS can be used to study the variety of valences present in a sample. In the single particle picture, the L_3 part (at 637 eV) and the L_2 part (at 648 eV) should have a 2 : 1 ratio and a similar spectral shape. In case of 3d-metals, multiplet effects completely dominate if a 2p- or a 3p-core hole is present. The 1s core hole is not affected by multiplet effects. This brings about a division into the soft X-ray edges, which are interpreted with multiplets, while the hard X-ray 1s edges are interpreted with single particle models. It is important for the remainder of the paper to realise that multiplet effects are a general phenomenon in case of 2p- or 3p-core holes are present in a 3d-metal. This implies that also the final states of X-ray emission, as used in site-selective XAFS experiments, are affected by multiplets. An important advantage of soft X-ray edges is their high resolution, which

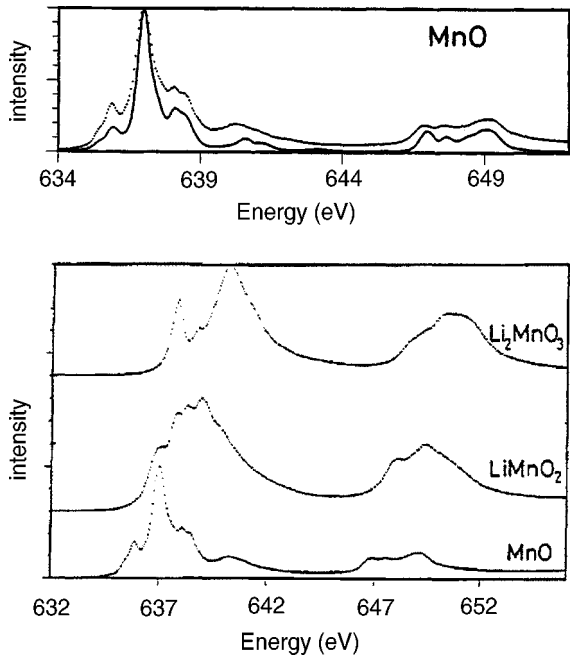

Figure 2. Top: the Mn 2p XANES spectrum of MnO, compared with a crystal field multiplet calculation (reproduced from [9]). Bottom: the 2p XANES spectrum of MnO (Mn^{2+}), $LiMnO_2$ (Mn^{3+}) and Li_2MnO_3 (Mn^{4+}).

can be less then 0.1 eV due to the long lifetime of the core states. This high resolution makes the spectra very sensitive to details of the electronic structure, such as the valence, the symmetry and spin state and the crystal field values [9].

A crucial feature of hard X-rays is their weak interaction with matter, allowing for bulk-sensitive measurements. It is possible to measure the X-ray absorption spectrum in a reaction cell at high pressure of high temperature. With the use of dispersive optical elements it is possible to detect all energies in a XAFS spectrum simultaneously. This allows for time-resolved studies that are essentially limited by the time needed to obtain the spectrum with acceptable signal to noise. Soft X-rays with energies below 2000 eV do interact strongly with matter. They penetrate less than a micrometer in matter and make (ultra-high) vacuum conditions obligatory. This limits their capability to do *in situ* measurements. The general picture is that soft X-rays are sensitive to details of the electronic and magnetic structure, but they cannot be used as *in situ* probes. It would be an important goal to create the possibility to do "soft X-ray experiments" *in situ*. How to do this will be described below.

The key to site-selective XAFS and the measurement of soft X-ray edges with hard X-rays lies in the various possibilities to measure the X-ray absorption spectral shape. The default detection technique of X-ray absorption spectra is transmission. The X-ray intensity is measured before and after the sample and the absorption coefficient is determined. Alternative detection techniques can be developed from the measurement of the core hole decay products. It can be shown that, with certain precautions, the total number of electrons as well as the total number of fluorescent X-rays is proportional to the X-ray absorption cross section. Both total electron yield (TEY) and total fluorescence yield (TFY) are often used. TEY is a very generally used technique, carried out under ultra-high vacuum (UHV) conditions. Complications can arise from the shallow escape depth and from the use of magnetic fields. TFY suffers from saturation and self-absorption effects. It can only be used if the edge absorption is a small portion of the total absorption (by nature or by dilution) [9]. If a valence state is used as the main source of the fluorescence, extra care should be taken [10]. Below it will be shown that the key to solve problems 1 and 2 lies in the use of special fluorescence channels. Before we go into that topic, first the X-ray emission (XES) spectral shapes will be discussed.

Once a deep core hole has been created, it decays and is filled by a shallow core or valence electron. The energy is emitted in the form of X-rays or, alternatively, another electron is emitted. The X-ray emission spectral shape is essentially given by the final state of the process, that is the state with the shallow core hole. This has been analysed in case of the nickel Kβ X-ray emission spectral shapes [11]. If the core hole is created with an energy close to an absorption edge, the X-ray absorption and X-ray emission processes do occur coherently and the overall process is described with the Kramers–Heisenberg formula:

$$I(\omega,\omega') \approx \sum_{\rm f} \left| \sum_{\rm x} \frac{\langle \Phi_{\rm f}|\hat{e}r|\Phi_{\rm x}\rangle\langle\Phi_{\rm x}|\hat{e}r|\Phi_{\rm i}\rangle}{\omega - E_{\rm x} - {\rm i}\Gamma_{\rm x}} \right|^2 \times \delta_{E_{\rm f}+\hbar\omega'-E_{\rm i}-\hbar\omega}. \quad (3)$$

This formula forms the basis of all resonant X-ray processes. The intensity (I) is given as a function of the excitation (ω) and the emission (ω') energies. The initial state ($\Phi_{\rm i}$) is excited to an intermediate state ($\Phi_{\rm x}$) with the dipole operator ($\hat{e}r$) and the second dipole operator ($\hat{e}'r$) describes the decay to the final state ($\Phi_{\rm f}$). The denominator contains the binding energy of the intermediate state ($E_{\rm x}$) and its lifetime broadening ($\Gamma_{\rm x}$). A resonance occurs if the excitation energy is equal to the binding energy of the intermediate state.

First we give a simple picture to explain why the lifetime broadening disappears. Figure 3 shows schematically the excitation of a 1s core electron at 3000 eV to the edge. One detects the 3p electrons that decay to the 1s hole. The life time broadening of the 1s level is chosen very large and the 3p level is chosen infinitely sharp. Then by putting the energy difference between excitation and decay exactly to 1000 eV, one detects only those electrons that go from to 3p level to the 1s level, following the 1s to edge excitation. In this process the broadening of the 1s level does not matter, for example, the two processes indicated by the arrows both are possible and are detected at the same energy difference $\omega' - \omega$. The exact description of the removal of the lifetime broadening is the Kramers–Heisenberg formula. Looking at this formula with figure 3 in mind, one can rewrite it by

assuming that there is no interference. This removes the denominator and gives

$$I(\omega)at[\omega-\omega'] \approx \sum_{\mathrm{f}}\sum_{\mathrm{x}} \left\langle \Phi_{\mathrm{f}}\middle|\hat{e}r\middle|\Phi_{\mathrm{x}}\right\rangle^2 \left\langle \Phi_{\mathrm{x}}\middle|\hat{e}r\middle|\Phi_{\mathrm{i}}\right\rangle^2 \times \delta_{E_{\mathrm{f}}+\hbar\omega'-E_{\mathrm{i}}-\hbar\omega}. \quad (4)$$

The summation of the X-ray emission matrix element yields a constant (I_{XES}) and can be removed from the formula. What remains is completely analogous to the normal XAFS (cf. equation (1)):

$$I(\omega)at[\omega-\omega'] \approx \sum_{\mathrm{x}} \left\langle \Phi_{\mathrm{x}}\middle|\hat{e}r\middle|\Phi_{\mathrm{i}}\right\rangle^2 \delta_{E_{\mathrm{f}}-E_{\mathrm{i}}-(\hbar\omega-\hbar\omega')}. \quad (5)$$

It can be seen that the matrix element concerns the intermediate state Φ_{x}, for example a 1s state, and the delta-function (that should be rewritten to a Lorentzian broadening) contains the final state and initial state, without the intermediate state. In other words the lifetime broadening of the intermediate state is completely removed from the experiment. This way of taking measurements will be written short-hand as $I_{\mathrm{XAS}}(\omega)|_{\omega'-\omega}$.

The general spectral "landscape" is a two-dimensional space with axes ω and ω'. A number of different cross sections can be made. One can measure the X-ray emission spectral shape with a particular fixed excitation energy. This will be indicated as $I_{\mathrm{XES}}(\omega')|_{\omega}$. If the excitation energy is (far) above a resonance this is normal X-ray emission or fluorescence. Close to a resonance, it is called *resonant X-ray emission.* Another cross section is to measure the X-ray absorption spectrum at a fixed emission energy: $I_{\mathrm{XAS}}(\omega)|_{\omega'}$. This experiment is not often performed though, and it is more usual to measure the X-ray absorption spectrum at a fixed energy difference between excitation and decay: $I_{\mathrm{XAS}}(\omega)|_{\omega'-\omega}$. This mode implies that the final state has a fixed binding energy and it is this mode that is used in site-selective XAFS, with the removal of the lifetime, as explained above [12].

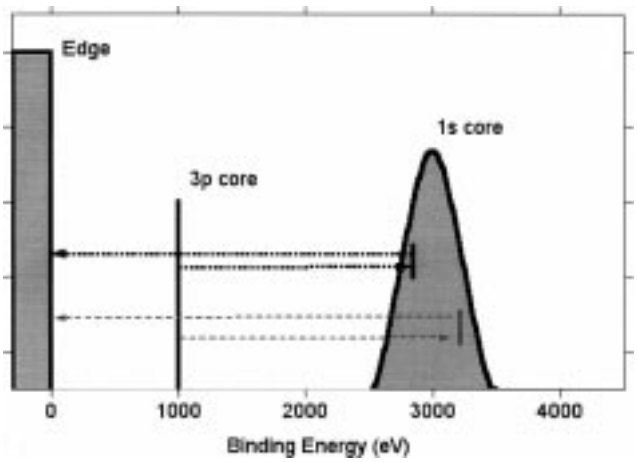

Figure 3. The removal of the lifetime broadening. An electron is excited from the broad 1s core level to the edge and a 3p electron fills the 1s hole. The detector is set at an energy $\omega'-\omega$, equal to the binding energy of the 3p state. In that case it does not matter if the top or bottom (virtual) transitions do take place (see text).

Yet another possibility is that one can study elementary excitations by probing the energy difference between the initial and final state: $I_{\mathrm{RIXS}}(\omega'-\omega)|_{\omega}$. This mode is known as *resonant inelastic X-ray scattering* (RIXS) and it can be used to study, for example, the dd-excitations in transition metals [13,14]. If one does not study valence excitations but core excitations, it is referred to as *X-ray Raman scattering* or *X-ray energy loss spectroscopy*. For example, one can measure the carbon K edge at 280 eV with X-rays of say 20 keV by detecting the X-rays with energies in between 19.6 and 19.8 keV. This process is the X-ray analogue to electron energy loss spectroscopy (EELS) and the resulting spectral shape identifies with X-ray absorption. As such, X-ray Raman scattering, is a straightforward way to measure soft X-ray spectra with hard X-rays. For clarity it is noted that X-ray Raman scattering is an extremely weak process, hence to actually perform these experiments one needs a very intense X-ray source [15]. We compare these three possibilities with normal X-ray absorption and X-ray emission in table 1.

As an example, the Kα X-ray emission spectra of Fe_2O_3 will be discussed. Figure 4 gives the Kα X-ray emission spectral shapes excited at the positions indicated with (a), (b) and (c). Additionally the off-resonant Kα spectrum is shown. The sharp and distinct features of the resonant Kα spectra are very similar to the 2p X-ray absorption spectral shape and they can be accurately simulated using a multiplet approach of the final state [16]. Figure 5 indicates the processes that do play a role in the simulation of the XES spectral shapes. The ground state of each Fe^{3+} ion has a half filled 3d shell and the excitations are both quadrupolar and dipolar. The quadrupole intermediate states have a $\underline{1s}3d^6$ configuration and the dipole intermediate states are $\underline{1s}3d^54p$. All decay channels are dipolar 1s2p and the final states are, respectively, $\underline{2p}3d^6$ and are $\underline{2p}3d^54p$. The X-ray absorption shows two pre-peaks (a) and (b) that can be related to, respectively, t_{2g} and e_g character states that are separated by the crystal field splitting. Because the decay process only involves the 1s and 2p core states, the character of the 3d states is maintained. This implies that if one measures the Kα X-ray emission spectrum at peak (a), one

Table 1
Comparison of different X-ray techniques.

$I_{\mathrm{XAS}}(\omega)$	X-ray absorption	Single monochromator for ω
$I_{\mathrm{XES}}(\omega')\|_{\omega\gg R}$	X-ray emission	Single monochromator for ω'
$I_{\mathrm{XES}}(\omega')\|_{\omega=R}$	Resonant X-ray emission	Two monochromators (ω and ω')
$I_{\mathrm{XAS}}(\omega)\|_{\omega'-\omega}$	Selective X-ray absorption	Two monochromators (ω and ω')
$I_{\mathrm{RIXS}}(\omega'-\omega)\|_{\omega}$	X-ray Raman scattering	Two monochromators (ω and ω')

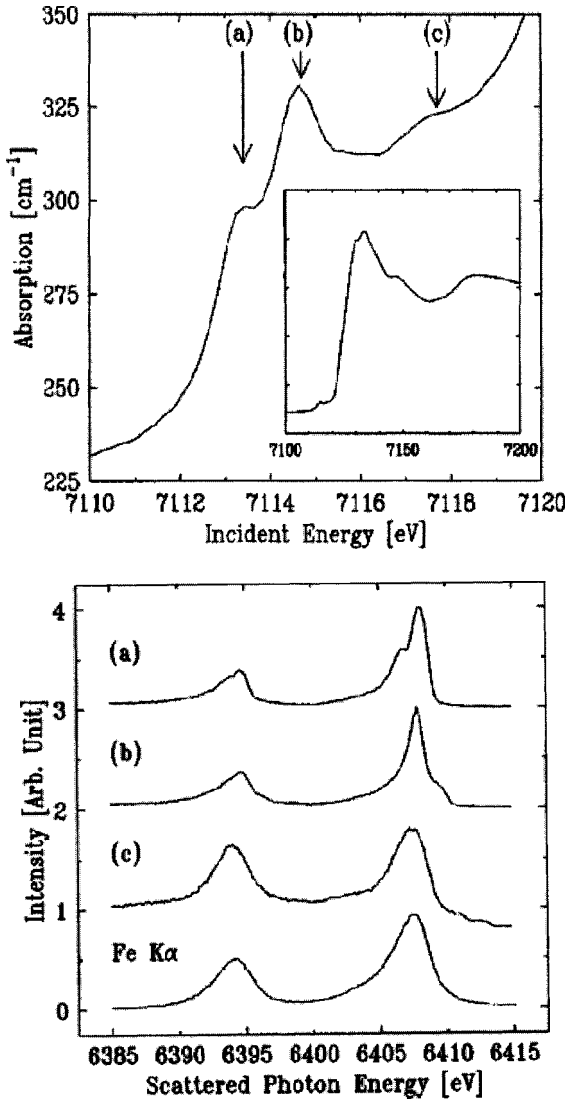

Figure 4. The bottom figure gives the Kα (1s2p) X-ray emission spectral shapes of Fe_2O_3. Spectra (a), (b) and (c) refer to the peak positions in the K edge X-ray absorption spectrum given at the top. (Reproduced from [16].)

obtains the t_{2g}-projected final states. Peak (b) yields the e_g-projected final states. Note that the final states reached via the quadrupole excitation are exactly the same as those of the 2p X-ray absorption. The 2p XAS spectral shape can be described as the transition from $3d^5$ to $\underline{2p}3d^6$. Thus from the resonant 1s2p XES spectral shape similar information can be obtained as from 2p XAS. This implies that the electronic structure and symmetry information of the shallow 2p state is obtained with the use of hard X-rays only, the excitation being at 7120 eV and the decay at 6400 eV. In other words this opens a way to do *in situ* hard X-ray experiments that are sensitive to the details of the electronic structure.

A related example is the Mn 1s3p (Kβ) X-ray emission spectrum of MnF_2. This spectrum is given on a log scale in figure 6. The Kβ' peak plus the K$\beta_{1,3}$ structure form together the actual 1s3p X-ray emission spectrum found

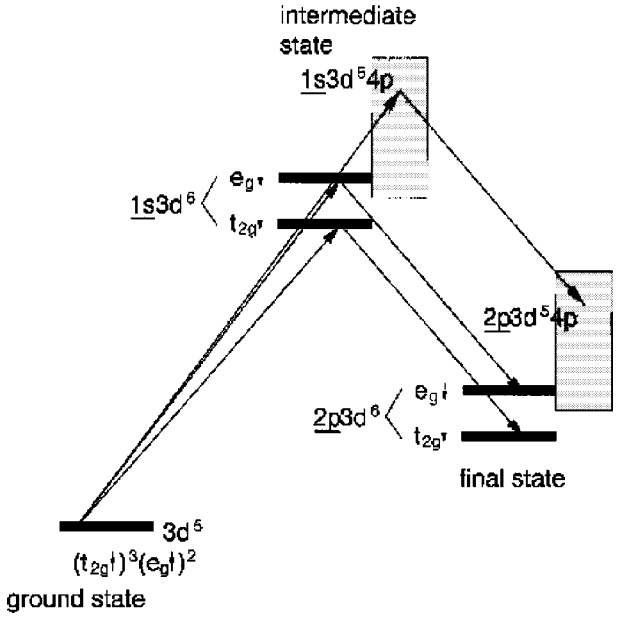

Figure 5. The ground state, intermediate states and final states in the resonant 1s2p X-ray emission spectral shapes.

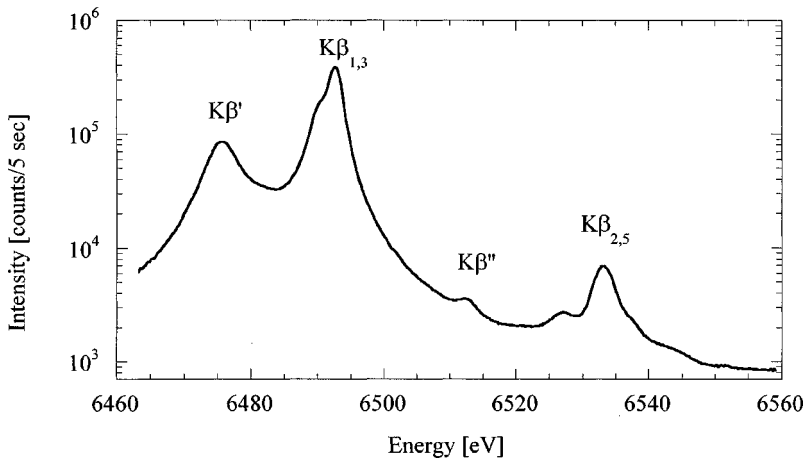

Figure 6. The Kβ (1s3p) and valence band X-ray emission spectral shapes of MnF_2. (Reproduced from [19].)

between 6470 and 6500 eV. It is split by the 3p3d multiplet effects [17]. Note that apart from the 1s3p X-ray emission spectral shape, some other weaker peaks are visible. The K$\beta_{2,5}$ structure is due to the valence band and the Kβ'' peak is due to the fluorine 2s states. Note that the valence band X-ray emission is some 10–100 times weaker than the 1s3p XES. Valence band XES is due to Mn 4p states that are hybridized with the fluorine 2p-valence band. It can be expected that additional intensity is due to quadrupole 3d1s decay from the five filled Mn 3d states. The valence band spectral shape seen in off-resonant 1s2p XES does relate to the valence band without the core hole. As such it should be related closely to valence band photoemission with some differences due to other selection rules. Measuring the valence band at resonance relates to resonant X-ray Raman scattering, which offers a whole range of new possibilities [14,18]. The weak fluorine 2s peak is also due to the Mn 4p character in this band. Note that this peak can be used as a probe of the amount of Mn 4p character in the F 2s band, hence of the amount of hybridization. As such it is a probe of the local Mn–F distance [19]. Thus both the valence band XES spectral shape as well as the peak position and intensity of shallow core states of neighbouring atom can provide two new tools to study the electronic (and magnetic) structure. Again, only hard X-rays are involved and *in situ* as well as time-resolved studies belong to the possibilities.

3. The use of particular fluorescence channels

Above we have seen that the combination of XAS and XES gives us a range of new hard X-ray tools to study the electronic structure and symmetry in great detail. At least seven different experiments can be distinguished:

(i) 1s2p and 1s3p XES, in particular resonant at the pre-edge peaks;

(ii) valence band XES, which essentially gives the valence band DOS;

(iii) cross-over XES, which provides information on the type of neighbouring atoms;

(iv) X-ray Raman scattering;

(v) using 1s2p or 1s3p XES (i) to remove the lifetime broadening in XAS;

(vi) using valence band energy shift in XES (ii) to measure valence-specific XAFS;

(vii) using cross-over XES (iii) to measure site-selective XAFS.

The central point of site-selective XAFS is to make use of a particular fluorescence channel to measure the X-ray absorption spectrum. For example, by measuring the X-ray absorption spectral shape at the peak positions of, respectively, the K$\beta_{1,3}$ and the Kβ' peaks, one can obtain the spin-selective X-ray absorption spectral shape [17,20]. This is important for the study of magnetic materials. It is well known that the fluorescence spectral shapes shift with increasing valence. One can tune the energy of the fluorescence detector to the peak position of one valence and vary the energy of the incoming X-ray, thereby measuring the XAFS spectrum of that particular valence. This can be repeated for the other valence. Consequently, one obtains separate XAFS spectra for the various valences present, in other words valence-selective X-ray absorption. An important point is that the whole experiment is carried out with hard X-rays. As shown above, the final state in the 1s2p and 1s3p processes has a 2p- or 3p-core hole that does interact strongly with the valence 3d electrons, creating a complex multiplet spectrum. This spectrum can be used as a fingerprint for the electronic structure. One arrives at the picture that the sensitivity of a shallow core level to the electronic structure/symmetry in the final state can be used to disentangle the XAFS spectra of the hard X-ray edges. This applies not only to the XANES region, but just as well to the EXAFS region, which allows for studies on the local geometry that are, for example, separated for their spin [21,22] or valence states [23].

Having described the basics of the experiment, it is necessary to say a few words about some practical points concerning the actual performance of the experiments. First of all the inelastic scattering processes are weak processes: only a (very) small percentage of the core holes created will decay at exactly the energy that is detected. The fluorescence goes in all directions and, because of the use of spherically bent crystal monochromators, the achievable solid angle is in the range of 0.1–1%. A practical complication is that the sub-eV energy resolution makes it necessary to work close to backscattering which puts strong limitations to the energy ranges that can be measured with a particular crystal. The consequence is that for each edge a different detector crystal must be used. Details on the X-ray optics involved can be found in [19].

4. Measuring only the active sites in *in situ* catalysts

A beautiful possibility arises from the F 2s to Mn 1s decay channel (Kβ'' in figure 6). This so-called cross-element resonant X-ray emission can be used to measure XAFS. Because the fluorine 2s peak is present only for the metal atoms that are neighbours to the fluorine, one can measure the XAFS spectra of only those metal atoms. It is important to note that the EXAFS analysis as such is essentially the same as for normal EXAFS and all atoms surrounding the excited atom do contribute to the electron scattering. Only the X-ray excitation and decay process is specific for one type of neighbour, while the electron scattering basis of EXAFS is not. It is important to note that the *non-local electron scattering* effects can be treated separately from the *local X-ray scattering* process.

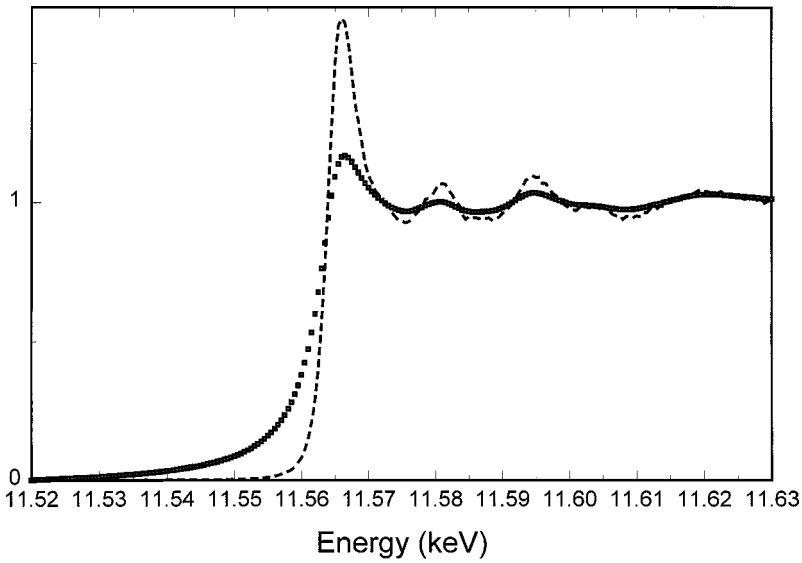

Figure 7. The platinum L_3 edge measured with fluorescence yield XAFS (points) and with Kα-detected XAFS (dashed).

Site-selective XAFS opens a large range of new series of experiments. The implications for three systems of the introduction are discussed below:

Concerning (i) the nickel nanoparticle supported on an oxide, one can use the oxygen 2s-emission channel to measure the nickel EXAFS spectra. In that case, only those nickel atoms in contact with oxygen (in the support) do contribute to the EXAFS signal. Another experiment would be to use the carbon emission channel and measure the nickel EXAFS. By doing so, one observes the local structure of those nickel atoms, which are in close contact with carbon, for example as a part of the transition state of a catalytic process. Provided a distinguishable cross-element fluorescence signal is present, one can use any combination of elements to do the experiment.

Concerning (ii), the Pt and Pd particles supported on oxides (zeolites, silica) or carbon fibrils, one can do the same experiment and use the oxygen 2s-emission channel to measure the Pt XAFS spectra. In case of Pt, one usually performs the XAFS analysis on the L_3 and L_2 edges. This implies that one is looking essentially at the "d" final states. It turns out to be the case that the cross-over peaks are less intense in that case. However, one can make use of one of the other new possibilities to improve upon the normal $L_{2,3}$ XAFS experiments. That is, one can remove the 2p lifetime broadening of some 4 eV, and replace it by the 3d or 4d lifetime broadening of less than 0.5 eV. This results in enormously sharper $L_{2,3}$ edges. Figure 7 shows the platinum L_3 edge with fluorescence yield XAFS (points) and with Kα-detected XAFS (dashed), both measured simultaneously at beamline ID26 at ESRF. Details on the experiment and the analysis will be published elsewhere. As predicted by equation (5), the L_3 is much sharper if the 2p lifetime broadening is removed. This sharpening makes it possible to measure the L_3 edge with very high resolution, provided the monochromator resolution is very good. The high-resolution XANES spectra can be used to study small variations in the lowest empty states (cf. equation (2)), which can become of great value to study the influence of, for example, H_2 or CO adsorption. Also the EXAFS spectrum will be sharper, and it can be expected that this will make possible a more accurate analysis.

Concerning (iii), the CoMo catalysts for HDS, one can use the oxygen 2s-emission channel to measure the Mo or the Co XAFS spectra. Only the Mo (or Co) atoms in contact with oxygen do contribute to the XAFS signal and one can study the Mo– and Co–support interactions in great detail. If the reaction is carried out with selenophene, Se binds to the active site and one can study the Mo (or Co) atoms in contact with Se, by measuring the Se-cross-over peak. By doing this experiment both for the Co and the Mo XAFS, one can immediately find the relative importance of the binding of Se to Co, respectively, Mo. Yet another option is, to check if is a decay channel specific to bound hydrogen, for example, the bonding combination of the metal–hydrogen bond in the valence band. If such channel would be found, it would create a new tool to study the important role of hydrogen, which is difficult to detect otherwise. The examples given present just a small portion of the wide range of possibilities from the various detection modes, as discussed above.

In conclusion it can be said that for any complex system that contains a range of elements in a variety of positions, site selective XAFS is able to strongly increase the amount of information over normal XAFS. Instead of the total average of all sites of the element studied, only those sites that are neighbours to another selected element do participate in the XAFS signal. Instead of this site selectivity, one can

also choose to remove the lifetime broadening or to use selectivity to the valence or in principle any effect that creates a difference in the X-ray emission spectral shapes. There is no fundamental limitation to use site selective XAFS to do *in situ* and time-resolved studies exactly like normal XAFS.

5. Outlook

It is our intention to develop site-selective XAFS as a versatile analytical tool for *in situ* studies of heterogeneous catalysts. Some questions that still have to be answered are the actual intensity limitations of site-selective XAFS, in particular of the EXAFS region. If these questions will be answered positively, site-selective XAFS will become a major *in situ* analytical tool for a large variety of systems.

Acknowledgement

I would like to thank Dr. Harry Bitter and Professor Diek Koningsberger for conversations. Figure 7 has been measured at beamline ID26 at ESRF, in collaboration with Dr. Michael Krisch. Figures 4 and 5 have been reproduced from [16] and figure 6 has been reproduced from [19].

References

[1] E. Boellaard, A.M. van der Kraan and J.W. Geus, Appl. Catal. A 147 (1996) 229.
[2] J. van de Loosdrecht, A.M. van der Kraan, A.J. van Dillen and J.W. Geus, Catal. Lett. 41 (1996) 27.
[3] B.L. Mojet and D.C. Koningsberger, Catal. Lett. 39 (1996) 191.
[4] D.E. Ramaker, B.L. Mojet, M.T.G. Oostenbrink, J.T. Miller and D.C. Koningsberger, Phys. Chem. Chem. Phys. 1 (1999) 2293.
[5] R.G. Leliveld, A.J. van Dillen, J.W. Geus and D.C. Koningsberger, J. Catal. 171 (1997) 115.
[6] R.G. Leliveld, A.J. van Dillen, J.W. Geus and D.C. Koningsberger, J. Catal. 175 (1998) 108.
[7] J.C. Fuggle and J.E. Inglesfield, eds., *Unoccupied Electronic States* (Springer, Berlin, 1992).
[8] J. Stöhr, *NEXAFS Spectroscopy* (Springer, Berlin, 1992).
[9] F.M.F. de Groot, J. Electron. Spectrosc. Relat. Phenom. 67 (1994) 529.
[10] F.M.F. de Groot, M.A. Arrio, P. Sainctavit, C. Cartier and C.T. Chen, Solid State Commun. 92 (1994) 991.
[11] F.M.F. de Groot, A. Fontaine, C.C. Kao and M.H. Krisch, J. Phys. Condens. Matter 6 (1994) 6875.
[12] K. Hämäläinen, D.P. Siddons, J.B. Hastings and L.E. Berman, Phys. Rev. Lett. 67 (1991) 2850.
[13] P. Kuiper, J.H. Guo, C. Sathe, J. Nordgren, J.J.M. Pothuizen, F.M.F. de Groot and G.A. Sawatzky, Phys. Rev. Lett. 80 (1998) 5204.
[14] F.M.F. de Groot, P. Kuiper and G.A. Sawatzky, Phys. Rev. B 57 (1998) 14584.
[15] M.H. Krisch, F. Sette, C. Masciovecchio and R. Verbeni, Phys. Rev. Lett. 78 (1997) 2843.
[16] W.A. Caliebe, C.C. Kao, J.B. Hastings, M. Taguchi, A. Kotani, T. Uozumi and F.M.F. de Groot, Phys. Rev. B 58 (1998) 13452.
[17] F.M.F. de Groot, S. Pizzini, A. Fontaine, K. Hamalainen, C.C. Kao and J.B. Hastings, Phys. Rev. B 51 (1995) 1045.
[18] J.P. Hill, C.C. Kao, W.A.L. Caliebe, M. Matsubara, A. Kotani, J.L. Peng and R.L. Greene, Phys. Rev. Lett. 80 (1998) 4967.
[19] U. Bergmann and S.P. Cramer, SPIE Proceedings 3448 (1998) 198.
[20] X. Wang, F.M.F. de Groot and S.P. Cramer, Phys. Rev. B 56 (1997) 4553.
[21] X. Wang and S.P. Cramer, J. Phys. IV 7 (1997) 361.
[22] X. Wang, C.R. Randall, G. Peng and S.P. Cramer, Chem. Phys. Lett. 243 (1995) 469.
[23] M.M. Grush, G. Christou, K. Hamalainen and S.P. Cramer, J. Am. Chem. Soc. 117 (1995) 5895.